RESEARCH PAPER

Synthesis and Characterization of Manganese Dioxide Nanoparticles for Drug Delivery Applications

Upasana Sarma[1]*, Dr. Sunandan Baruah[2], Dr. Sanjib Karmakar[3], Nairika Deka[4], Pranjal Sarma[5]

[1]Gauhati University, Jalukbari, Assam
[2]Assam Skill University, Mangaldai, Assam
[3]Gauhati University, Jalukbari, Assam
[4]Assam Down Town University, Panikhaiti, Assam.
[5]Assam Don Bosco University, Guwahati, Assam

Abstract

Manganese dioxide (MnO_2) nanoparticles have attracted considerable attention in nanomedicine because of their unique physicochemical properties, excellent biocompatibility, catalytic activity and responsiveness to the tumor microenvironment. These characteristics make MnO_2 nanoparticles a promising candidate for targeted drug delivery, bioimaging and cancer therapy. In the present study, MnO_2 NPs were synthesized by a simple chemical precipitation method using manganese acetate as the precursor and sodium hydroxide as the precipitating agent. The synthesized nanoparticles were characterized using ultraviolet-visible (UV-Vis) spectroscopy, X-ray diffraction (XRD) and transmission electron microscopy (TEM) to evaluate their optical properties, crystalline structure and morphology. The characterization results confirmed the successful formation of crystalline MnO_2 nanoparticles with nanoscale dimensions. Owing to their ability to degrade under acidic and glutathione-rich conditions, MnO_2 nanoparticles function as stimuli-responsive drug carriers, enabling controlled drug release specifically within the tumor microenvironment.

Keywords: Manganese dioxide nanoparticles, Drug delivery, Nanomedicine, X-ray diffraction, Transmission electron microscopy, UV-Visible spectroscopy, Tumor microenvironment Responsiveness, Theranostics.

How to cite this article: Sarma U, Baruah S, Karmakar S, Deka N, Sarma P. Synthesis and Characterization of Manganese Dioxide Nanoparticles for Drug Delivery Applications. Int J Drug Deliv Technol. 2026;16(69s): 1747-1751. DOI: 10.25258/ijddt.16.69s.173

1. Introduction

Nanotechnology has emerged as one of the most rapidly advancing fields in biomedical science, providing innovative approaches for disease diagnosis, imaging and targeted drug delivery **[1–5]**. Nanoparticles possess unique physicochemical properties including a high surface-area-to-volume ratio, tunable surface chemistry and enhanced catalytic activity, making them highly suitable for pharmaceutical and biomedical applications **[1,3, 23,24]**. Among the various inorganic nanomaterials investigated for therapeutic applications, manganese dioxide (MnO_2) nanoparticles have attracted significant attention because of their multifunctional characteristics and excellent biocompatibility **[6–13]**.

Manganese is a transition metal that exhibits oxidation states ranging from −3 to +7, with +2 and +4 being the most thermodynamically stable under physiological conditions. The multiple oxidation states of manganese enable extensive redox chemistry, allowing manganese oxides to participate in various oxidation–reduction reactions [12,21]. Among the different manganese oxides, manganese dioxide (MnO_2), containing manganese in the +4 oxidation state, is particularly important because of its excellent catalytic activity, oxidizing capability, chemical stability, and environmental compatibility **[12,14,21].**

MnO_2 nanoparticles have been extensively investigated for applications in lithium-ion batteries, supercapacitors, catalysis, environmental remediation, biosensing, magnetic resonance imaging (MRI), and drug delivery **[6–14]**. Depending on the synthesis conditions, MnO_2 exists in several crystallographic polymorphs, including α-, β-, γ-, and δ-MnO_2, each possessing distinct crystal structures and physicochemical properties that influence their functional performance **[12,14–16]**. Consequently, the synthesis route plays a crucial role in determining particle morphology, crystallinity, and biomedical applicability **[12,15,16]**.

Recent advances in nanomedicine have demonstrated that MnO_2 nanoparticles can function as intelligent, stimuli-responsive drug carriers. Unlike conventional drug delivery systems, MnO_2 nanoparticles remain stable under normal physiological conditions (pH ≈ 7.4) but readily decompose within the acidic and glutathione-rich tumor microenvironment **[6–13]**.

The degradation of MnO_2 nanoparticles is primarily governed by intracellular glutathione (GSH), which is present at significantly higher concentrations in cancer

*Author for Correspondence: Upasana Sarma

cells than in normal tissues **[6,7,12,13].** The reduction of MnO_2 can be represented by the following reaction:

$$2MnO_2 + GSH + 4H^+ \rightarrow 2Mn_2 + GSSG + 2H_2O$$

The generated Mn^{2+} ions not only facilitate drug release but also serve as effective T_1-weighted magnetic resonance imaging (MRI) contrast agents, enabling simultaneous diagnosis and therapy **[7,12,13].** This dual functionality has established MnO_2 nanoparticles as promising theranostic agents **[6,7,12,13].**

Another important advantage of MnO_2 nanoparticles is their ability to overcome tumor hypoxia. Solid tumors typically exhibit low oxygen levels, which significantly reduce the effectiveness of chemotherapy, radiotherapy, and photodynamic therapy **[8,12,13]**. MnO_2 nanoparticles react with endogenous hydrogen peroxide (H_2O_2), which is over expressed in tumor tissues, to generate molecular oxygen according to the following reaction **[8,12]**:

$$2MnO_2 + 2H_2O_2 \rightarrow O + 2Mn^{++} + 4OH^-$$

The generated oxygen improves the oxygenation of tumor tissues, thereby enhancing the efficacy of conventional cancer therapies. Simultaneously, the released Mn^{2+} ions enable MRI-guided monitoring of nanoparticle accumulation and X_c response **[8,12,13]**.

Various synthesis methods have been reported for the preparation of MnO_2 nanoparticles, including hydrothermal synthesis, sol-gel processing, chemical precipitation, microwave-assisted synthesis and oxidation-reduction techniques. Among these, the chemical precipitation method is particularly attractive because it is simple, economical, environmentally friendly and suitable for large-scale production.

In the present work, MnO_2 nanoparticles were synthesized by a chemical precipitation method using manganese acetate and sodium hydroxide as precursor materials. The synthesized nanoparticles were characterized using UV-Visible spectroscopy and X-ray diffraction (XRD) to investigate their optical, structural, and morphological properties.**[15–20]** Furthermore, the potential application of these nanoparticles as stimuli-responsive drug delivery systems is discussed based on their physicochemical characteristics and recent developments in nanomedicine. **[2,12,22–24]**

2. Materials and Methods

2.1 Materials

Analytical-grade manganese acetate tetrahydrate [$Mn(CH_3COO)_2 \cdot 4H_2O$] and sodium hydroxide (NaOH) were used as the starting materials for the synthesis of manganese dioxide (MnO_2) nanoparticles. All chemicals were of analytical reagent (AR) grade and were used without further purification. Double-distilled water was used throughout the synthesis.

2.2 Synthesis of Manganese Dioxide Nanoparticles

MnO_2 nanoparticles were synthesized using a simple chemical precipitation method. Initially, **20 mL of 4 mM manganese acetate solution** was prepared and stirred continuously using a magnetic stirrer at **50 °C** for **45 min** to obtain a homogeneous solution.

A freshly prepared sodium hydroxide solution was then added dropwise to the manganese acetate solution under constant stirring. The reaction mixture was stirred continuously for **1 h**, allowing complete precipitation of manganese oxide nanoparticles.

The resulting suspension was subsequently heated in a water bath maintained at **60–80 °C** for approximately **1h** to promote particle growth and improve crystallinity. After completion of the reaction, the precipitate was separated by centrifugation and washed several times with distilled water to remove residual ions and unreacted precursors. The purified precipitate was dried in a hot-air oven at **60 °C** until a constant weight was obtained. The dried powder was collected and stored in an airtight container for further characterization.

2.3 Characterization of MnO_2 Nanoparticles

The synthesized MnO_2 nanoparticles were characterized using different analytical techniques to investigate their structural, optical, and morphological properties.

2.3.1 UV–Visible Spectroscopy

The optical properties of the synthesized nanoparticles were analyzed using a UV–Visible spectrophotometer over an appropriate wavelength range. The absorption spectrum was recorded to identify the characteristic absorption peak of MnO_2 nanoparticles. The obtained absorbance data were used to estimate the optical band gap using the Tauc relation, which provides valuable information regarding the electronic structure of the nanoparticles **[6,12,17,20].**

The optical band gap (Eg) was determined using the following equation **[17]**:

$$(\alpha hv)\text{^}(1/n) = A(hv - E_g)\ )$$

Rearranging specifically for the x-intercept where absorption becomes zero ($\alpha = 0$)

$$E_g = h/v$$

where:
α is the absorption coefficient
h is Planck's constant
ν is the frequency of incident radiation
Eg is the optical band gap
A is a proportionality constant
n depends on the nature of the electronic transition.

The UV–Visible spectrum also provides indirect information regarding particle size and confirms the successful formation of MnO_2 nanoparticles **[6,12,20]**.

2.3.2 X-ray Diffraction (XRD)

The crystalline structure and phase purity of the synthesized nanoparticles were investigated using X-ray diffraction (XRD) analysis. Diffraction patterns

were recorded using a **Rigaku X-2500 X-ray diffractometer** equipped with **Cu K_α radiation (λ = 1.5406 Å)**.
The observed diffraction peaks were indexed according to standard Joint Committee on Powder Diffraction Standards (JCPDS) data to confirm the formation of crystalline MnO_2. The average crystallite size (D) was estimated using the Debye–Scherrer equation:
$D = K\lambda/\beta\cos\theta$
where:

- D = crystallite size
- K = shape factor (0.9)
- λ = wavelength of X-rays,
- β = full width at half maximum (FWHM),
- θ = Bragg diffraction angle.

The XRD analysis provides information regarding crystal structure, crystallite size and phase composition of the synthesized nanoparticles.

MnO_2 nanoparticles have emerged as promising smart nanocarriers for targeted drug delivery because of their responsiveness to the unique physiological conditions of the tumor microenvironment. Unlike conventional nanocarriers, MnO_2 nanoparticles remain relatively stable under normal physiological conditions (pH ≈ 7.4) but readily degrade in the acidic and glutathione-rich environment of tumor tissues.

3.1 Stimuli-Responsive Drug Release
Cancer cells contain significantly higher concentrations of glutathione (GSH) than normal cells. In the presence of GSH and acidic pH, MnO_2 nanoparticles undergo reduction to produce soluble Mn^{2+} ions, resulting in the degradation of the nanoparticle shell and controlled release of the encapsulated therapeutic drug.
The reduction reaction can be represented as **[6,7,12,13]:**

$$2MnO_2+GSH+4H^+ \rightarrow 2Mn^2+GSSG+2H_2O$$

This mechanism minimizes premature drug leakage during circulation while ensuring site-specific drug release at the tumor location **[6,7,12].**

3.2 Oxygen Generation for Hypoxia Relief
Hypoxia is a major limitation in cancer therapy because oxygen-deficient tumor tissues exhibit poor responses to chemotherapy, radiotherapy, and photodynamic therapy **[8,12,13]**. MnO_2 nanoparticles react with endogenous hydrogen peroxide (H_2O_2), which is abundant in tumor tissues, producing molecular oxygen according to the following reaction **[8,12]**:

$$2MnO_2+2H_2O_2+2Mn^{2+}+4OH^-$$

The generated oxygen alleviates tumor hypoxia and significantly enhances the therapeutic efficiency of conventional anticancer treatments **[8,12,13]**.

3.3 MRI-Guided Theranostic Applications
During degradation, MnO_2 nanoparticles release Mn^{2+} ions, which serve as efficient T_1-weighted magnetic resonance imaging (MRI) contrast agents. Consequently, MnO_2 nanoparticles enable simultaneous drug delivery and real-time imaging, allowing clinicians to monitor nanoparticle accumulation and therapeutic response. This combination of diagnosis and therapy, commonly referred to as **theranostics**, represents one of the most promising biomedical applications of MnO_2 nanomaterials.

4.1 Results and Discussion
4.1.1 UV–Visible Spectroscopy
The UV–Visible absorption spectrum of the synthesized MnO_2 nanoparticles exhibited a broad absorption band in the ultraviolet region, confirming the successful formation of manganese dioxide nanoparticles. The broad absorption is attributed to charge transfer transitions between Mn and O atoms within the MnO_2 lattice. The absence of additional absorption peaks indicates that the synthesized product was free from significant impurities **[6,12,20]**.
The optical band gap was estimated using the Tauc plot. **[17]** Extrapolation of the linear portion of the curve to the energy axis yielded the optical band gap of the synthesized nanoparticles. The observed band-gap value falls within the range commonly reported for nanocrystalline MnO_2, indicating the semiconducting nature of the material. The nanoscale dimensions of the particles contribute to slight band-gap modification due to quantum confinement effects **[6,12,17]**.

X-ray Diffraction (XRD) Analysis
The X-ray diffraction (XRD) pattern of the synthesized MnO_2 nanoparticles is shown in **Figure 1**. The diffraction pattern exhibits distinct diffraction peaks at approximately **18°, 30°, 35°, and 60° (2θ)**, corresponding to the crystallographic planes indexed as **(200), (310), (211), and (521)**, respectively. The presence of these diffraction peaks confirms the successful formation of crystalline manganese dioxide nanoparticles.
The diffraction peaks are relatively broad, indicating that the synthesized particles possess nanocrystalline dimensions. Peak broadening is commonly associated with the small crystallite size of nanoparticles and may also be influenced by lattice strain. No prominent diffraction peaks corresponding to impurity phases were observed, suggesting that the synthesized sample possesses good phase purity**[15,16].**
The average crystallite size can be estimated using the Debye–Scherrer equation**[15,16,18]**:

$$D=K\lambda/\beta\cos\theta$$

where D is the crystallite size, K is the shape factor (0.9), λ is the wavelength of Cu Kα radiation (1.5406 Å), β is the full width at half maximum (FWHM), and θ is the Bragg diffraction angle. Since the FWHM values were not extracted from the diffraction data, the crystallite size was not calculated in the present study.

The obtained XRD results confirm that the chemical precipitation method successfully produced crystalline MnO_2 nanoparticles suitable for further investigation as stimuli-responsive drug delivery nanocarriers. **[6,7,12,13]**

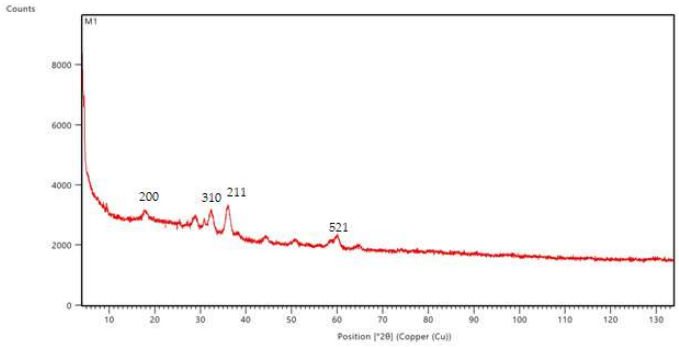

Figure 1. X-ray diffraction pattern of the synthesized MnO_2 nanoparticles showing characteristic diffraction peaks corresponding to crystalline manganese dioxide

Conclusion

MnO_2 nanoparticles were successfully synthesized using a simple and cost-effective chemical precipitation method employing manganese acetate and sodium hydroxide as precursor materials. Characterization by UV–Visible spectroscopy, X-ray diffraction, and transmission electron microscopy confirmed the successful formation of crystalline MnO_2 nanoparticles with nanoscale dimensions. The synthesized nanoparticles exhibited favorable optical and structural properties suitable for biomedical applications **[12,15–20]**.

The unique responsiveness of MnO_2 nanoparticles to the acidic and glutathione-rich tumor microenvironment enables controlled drug release specifically at the target site, thereby reducing systemic toxicity **[3,6,7,10,12,13]**. Furthermore, their catalytic ability to generate oxygen from endogenous hydrogen peroxide alleviates tumor hypoxia, while the release of Mn^{2+} ions provides MRI contrast enhancement for image-guided therapy **[6–8,12,13]**. These multifunctional characteristics make MnO_2 nanoparticles promising candidates for advanced drug delivery and theranostic applications **[2,6–8,12,13,23,24]**. Future studies involving drug-loading efficiency, *in vitro* cytotoxicity, cellular uptake, and *in vivo* therapeutic evaluation will further establish their potential for clinical translation **[2,4,23–25]**.

References

1. Peer D, Karp JM, Hong S, Farokhzad OC, Margalit R, Langer R. Nanocarriers as an emerging platform for cancer therapy. Nat Nanotechnol. 2007;2(12):751–60.
2. Shi J, Kantoff PW, Wooster R, Farokhzad OC. Cancer nanomedicine: progress, challenges and opportunities. Nat Rev Cancer. 2017;17(1):20–37.
3. Torchilin VP. Multifunctional and stimuli-sensitive pharmaceutical nanocarriers. Eur J Pharm Biopharm. 2009;71(3):431–44.
4. Wilhelm S, Tavares AJ, Dai Q, Ohta S, Audet J, Dvorak HF, et al. Analysis of nanoparticle delivery to tumours. Nat Rev Mater. 2016;1:16014.
5. Fang J, Nakamura H, Maeda H. The EPR effect: unique features of tumour blood vessels for drug delivery. Adv Drug Deliv Rev. 2011;63(3):136–51.
6. Lin LS, Song J, Song L, Ke K, Liu Y, Zhou Z, et al. Simultaneous Fenton-like ion delivery and glutathione depletion by MnO_2-based nanoagent to enhance chemodynamic therapy. Angew Chem Int Ed Engl. 2018;57(18):4902–6.
7. Chen Y, Ye D, Wu M, Chen H, Zhang L, Shi J, et al. Break-up of two-dimensional MnO_2 nanosheets promotes ultrasensitive pH-triggered theranostics of cancer. Adv Mater. 2014;26(41):7019–26.
8. Fan H, Yan G, Zhao Z, Hu X, Zhang W, Liu H, et al. A smart photosensitizer–manganese dioxide nanosystem for enhanced photodynamic therapy by reducing tumour hypoxia. Angew Chem Int Ed Engl. 2016;55(18):5477–82.
9. Zhen X, Zhang C, Xie C, Miao Q, Lim KL, Pu K. Intraparticle energy level modulation of semiconducting polymer nanoparticles augments photoacoustic imaging and photothermal therapy. ACS Nano. 2016;10(6):6400–9.

10. Liu J, Huang Y, Kumar A, Tan A, Jin S, Mozhi A, Liang XJ. pH-sensitive nano-systems for drug delivery in cancer therapy. Biotechnol Adv. 2014;32(4):693–710.
11. Estelrich J, Busquets MA. Iron oxide nanoparticles in photothermal therapy. Molecules. 2018;23(7):1567.
12. Sun H, Zhang B, Jiang J, Li X, Wu Y, Chen Y. Manganese dioxide nanoparticles as responsive nanocarriers for cancer theranostics. J Mater Chem B. 2019;7:2865–79.
13. Wang Y, Zhang K, Qin X, Li T, Qiu J, Yin T, et al. Biomimetic MnO_2 nanoparticles for enhanced tumor therapy and magnetic resonance imaging. ACS Appl Mater Interfaces. 2019;11(51):47671–82.
14. Goodenough JB, Kim Y. Challenges for rechargeable Li batteries. Chem Mater. 2010;22(3):587–603.
15. Cullity BD, Stock SR. Elements of X-ray Diffraction. 3rd ed. Upper Saddle River (NJ): Prentice Hall; 2001.
16. Klug HP, Alexander LE. X-ray Diffraction Procedures for Polycrystalline and Amorphous Materials. 2nd ed. New York: Wiley; 1974.
17. Tauc J. Optical properties and electronic structure of amorphous germanium. Mater Res Bull. 1968;3(1):37–46.
18. Patterson AL. The Scherrer formula for X-ray particle size determination. Phys Rev. 1939;56(10):978–82.
19. Williams DB, Carter CB. Transmission Electron Microscopy: A Textbook for Materials Science. 2nd ed. New York: Springer; 2009.
20. Skoog DA, Holler FJ, Crouch SR. Principles of Instrumental Analysis. 7th ed. Boston: Cengage Learning; 2018.
21. IUPAC. Compendium of Chemical Terminology (Gold Book). 2nd ed. Oxford: Blackwell Scientific Publications; 1997.
22. Roco MC. Nanotechnology: convergence with modern biology and medicine. Curr OpinBiotechnol. 2003;14(3):337–46.
23. Shi J, Votruba AR, Farokhzad OC, Langer R. Nanotechnology in drug delivery and tissue engineering: from discovery to applications. Nano Lett. 2010;10(9):3223–30.
24. Farokhzad OC, Langer R. Impact of nanotechnology on drug delivery. ACS Nano. 2009;3(1):16–20.
25. De Jong WH, Borm PJA. Drug delivery and nanoparticles: applications and hazards. Int J Nanomedicine. 2008;3(2):133–49.